Nonlinear numerical modelling of complex masonry heritage structures considering history-related phenomena in staged construction analysis and material uncertainty in seismic assessment

Savvas Saloustros[a], Luca Pelà[b*], Pere Roca[c]

[a]Research Fellow, Department of Civil and Environmental Engineering, Universitat Politècnica de Catalunya (UPC-BarcelonaTech), Jordi Girona 1-3, 08034 Barcelona, Spain. E-mail: savvas.saloustros@upc.edu

[b]Associate Professor, Department of Civil and Environmental Engineering, Universitat Politècnica de Catalunya (UPC-BarcelonaTech), Jordi Girona 1-3, 08034 Barcelona, Spain (*corresponding author). E-mail: luca.pela@upc.edu

[c]Professor, Department of Civil and Environmental Engineering, Universitat Politècnica de Catalunya (UPC-BarcelonaTech), Jordi Girona 1-3, 08034 Barcelona, Spain. E-mail: pere.roca.fabregat@upc.edu

ABSTRACT

This paper presents the systematic use of numerical analysis as a tool for addressing some of the most common challenges encountered in the structural analysis of complex historical masonry structures, i.e. the description of the effects of history-related phenomena and the uncertainty of material properties. The numerical strategy is based on the use of a constitutive model able to describe time-dependent strain accumulation, as well as damaging behaviour under different stress states. This constitutive model is combined with a crack-tracking technique

ORCID: 0000-0002-9513-8373 (Savvas Saloustros), 0000-0001-7760-8290 (Luca Pelà), 0000-0001-5400-5817 (Pere Roca)

to represent tensile crack localization. The numerical model is applied to the study of two important monuments in Spain, i.e. the Mallorca Cathedral and the church of the Poblet Monastery. The staged construction analysis of the first case study allows understanding the reasons of its current deformed condition, i.e. critical construction process, strain accumulation given by long-term creep phenomena, and nonlinear geometric effects. The structural analysis of the second case study allows the structural diagnosis of the existing deformation and cracking patterns given by architectural alterations, insufficient buttressing of the naves, and past earthquakes. The application of a probabilistic analysis to the church of the Poblet monastery allows considering the effects of the uncertainties of material properties and numerical parameters in the seismic vulnerability assessment.

Keywords: Historical masonry structures; continuum damage mechanics; visco-elasticity; crack-tracking; earthquakes; Monte-Carlo simulation; probabilistic analysis; stochastic analysis; pushover.

INTRODUCTION

The study of structures declared as built cultural heritage requires a multidisciplinary approach [1,2]. Historical research, inspection (including experiments), monitoring and structural analysis are different stages of the so-called scientific method for the structural assessment of the architectural heritage. The first three activities can provide essential information (real data) to build and calibrate the structural model. At the same time, they allow the validation of the structural analysis results by comparison with empirical evidence. The structural model is the recipient of the analyst's hypotheses, and the process of calibrating/validating is the direct result of the application of the scientific method. This interdisciplinary framework allows drawing optimal conclusions, such as diagnosis of the current condition of the structure, evaluation of

the safety level and design of optimum interventions respectful of the heritage value of the structure.

Structural modelling and analysis of complex historical structures face several challenges. These structures commonly present a complex geometry resulting from the combination of different types of structural members, such as columns, arches, vaults, domes, buttresses, etc. Such elements may present either massive or slender character. Today, numerical models, such as those based on Finite Element Method (FEM), can afford a realistic and accurate description of geometry, even though the pre-processing stage can be rather challenging. A direct consequence of the complex geometry of historical constructions is the generation of laborious numerical models, involving a large number of nodes, elements and thus equations to be solved. Consequently, the structural model needs to be a compromise between realism and computational cost.

Another important challenge in the structural modelling of existing structures, apart from the geometry, are historical events that have normally left evidence on the structures. For instance, historical structures may present important deformations and damage related to a critical construction process, architectural alterations or additions [3], anthropogenic damage or partial destruction during conflicts and fires, effects of natural hazards (such as earthquakes, floods) [4–9], soil settlements [10–13], long-term damage phenomena [14–16], or a combination of more than one events. For this, structural analysis should be planned considering past events identified by the historical survey that could have potentially affected the investigated structure.

A large percentage of historical structures is made of stone or brick masonry. This composite and heterogeneous material is characterized by variability and lack of standardization, as a large number of combinations of components are possible (units and mortars), as well as

materials (stone, brick, lime, etc.), dimensions of constituents, arrangement of units, and building techniques. In addition, masonry has an extremely complex mechanical behavior, with quasi-brittle character in tension and limited ductility in compression, nonlinearity of stress-strain relationship, frictional response in shear, and anisotropy.

It becomes clear from the above that modelling of masonry structures is not straightforward. For this reason, different types of computational strategies based on the FEM are available in the scientific literature [17–19], ranging from micromodels including the discretization of units and joints (e.g. [20,21]), to macromodels representing the material from a phenomenological point of view as a homogenized equivalent continuum (e.g. [22–25]. A recent approach is also multiscale modelling [26], in which the macroscale (at the level of structure) exchanges information with the microscale (at the level of a representative volume element of the material) during the analysis. Both micromodelling and multiscale modelling are characterized by a remarkable computational cost, making them still inadequate for the analysis of complex historical constructions [17]. While the continuous advance of the capacity of personal computers will make eventually these approaches more accessible to analysts, today, the use of macromodels seems the most adequate approach to deal with the analysis of this type of structures.

During the last decades, the increasing application of numerical analysis in the study of historical structures has contributed to our better understanding of their structural behavior. For instance, the application of advanced numerical models is of paramount importance to simulate the long-term stability of historical constructions made of masonry, as time-dependent effects may induce cumulative damage and deformation degenerating into collapse, as demonstrated by past events, e.g. the collapses of Pavia Civic Tower in 1989 and Noto Cathedral in 1996 [27]. FEM macromodels are also very useful to simulate the structural collapse condition in case of earthquake in order to evaluate the seismic safety, as historical structures show to be

very vulnerable to these type of events as proved by recent earthquakes, e.g. L'Aquila 2009, Emilia Romagna 2012, Central Italy 2016, Lesvos 2017 [28,29].

On the other hand, it is important to recognize that numerical models are commonly based on two strong assumptions. The first assumption is related to the adoption of deterministic values for the material properties (e.g. tensile and compressive strength, Young's modulus, etc.). This is a controversial choice considering the composite and heterogeneous nature of masonry, which depends on workmanship and can present high variability—even within the same structure—due to weather conditions, past damage and time-deterioration. The second assumption is related to the adoption of a specific numerical model (i.e. constitutive relationship, numerical formulation, etc.) for the representation of the physical behavior of the simulated material. Each numerical model is commonly based on numerical parameters that cannot be experimentally calibrated. These assumptions present various sources of uncertainties that may influence the conclusions of the structural analysis and consequently the choices of the intervention strategy.

This manuscript deals with the application of FE macromodelling analysis for the structural assessment of complex historical masonry structures against long-term deformation, past historical alterations and seismic actions. The paper is composed of three parts. The first part is devoted to the presentation of a FEM model based on continuum mechanics theory able to reproduce from a macroscopic phenomenological point of view some of the history-related mechanical phenomena typically encountered in masonry structures, i.e. time-dependent strain accumulation due to viscous effects, orthotropy and tensile crack localization. The second part presents two applications of the FEM on two important monuments in Spain: the cathedral of Mallorca and the church of the Poblet monastery. The third part includes a probabilistic analysis for assessing the effect of uncertainties related with material and numerical properties on the seismic response of the church of the Poblet monastery.

MECHANICAL MODEL FOR MASONRY

The proposed mechanical model for masonry is able to simulate the time-dependent strain accumulation in the material because of long-term exposure to constant stress, including the description of tensile and compressive damage. The main idea of the viscous model is the representation of the time-dependent deformation through a time-dependent stiffness defined by two components, i.e. a constant one and a viscosity susceptible one [30]. Figure 1 shows the uniaxial rheological model represented by two elements in parallel, consisting respectively of a Hookean spring, and a Maxwell chain with a spring in series with a dashpot. The elastic stiffness of the first spring is E_∞, that of the second spring is E_v and the viscosity parameter η is the term of proportionality between the viscous stress in the dashpot and the viscous strain rate $\sigma_v = \eta \dot{\varepsilon}_v$. The dashpot is infinitely stiff at the beginning of the deformation process, while its stiffness tends to zero for infinite time. The initial stiffness of the system is given by the sum of the stiffness of the two springs ($E_0 = E_\infty + E_v$). The stiffness of the system for $t = +\infty$ is equal to E_∞, due to the dashpot's complete relaxation at the end of the deformation process. The total stress sustained by the system is:

$$\sigma = \sigma_e + \sigma_v = E_\infty \varepsilon + \xi E_0 \left(\varepsilon - \varepsilon_v \right) \tag{1}$$

where ε represents the total deformation of the system, ε_v denotes the viscous strain of the chain increasing with time under a constant stress σ, and $\xi = E_v / E_0$ is the participation ratio defining the amount of stiffness susceptible to viscosity. The retardation time $\vartheta = \eta / E_v$ defines the time scale of the viscous phenomenon, as it is linked to the time required for dashpot relaxation (rate of viscous strain). The strain rate of the system is:

$$\dot{\varepsilon} = \frac{\dot{\sigma}_v}{E_v} + \frac{\sigma_v}{\eta} \tag{2}$$

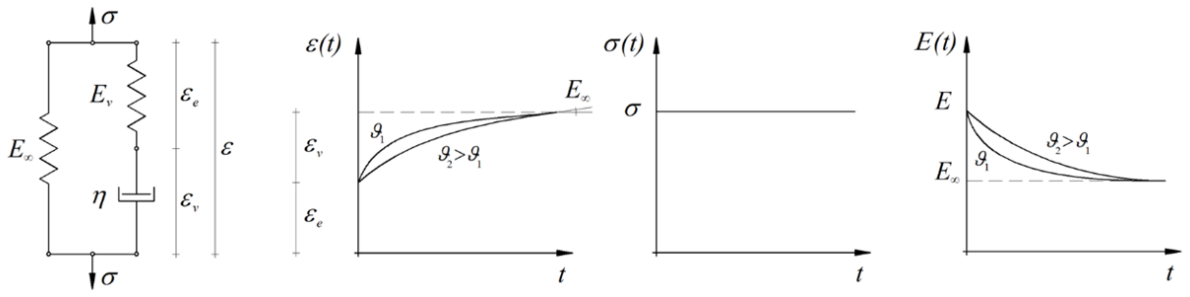

Figure 1: Uniaxial rheological viscous model [30]

In the multidimensional case, Equation 2 is rewritten as follows:

$$\xi \mathbf{C} : \dot{\boldsymbol{\varepsilon}} = \dot{\boldsymbol{\sigma}}_v + \frac{\boldsymbol{\sigma}_v}{\vartheta} \tag{3}$$

Assuming the viscous strain in the Maxwell chain $\boldsymbol{\sigma}_v = \xi \mathbf{C} : \left(\boldsymbol{\varepsilon} - \boldsymbol{\varepsilon}_v \right)$ as internal variable, the evolution law for the viscous strain is:

$$\dot{\boldsymbol{\varepsilon}}_v = \frac{1}{\vartheta} \left(\boldsymbol{\varepsilon} - \boldsymbol{\varepsilon}_v \right) \tag{4}$$

The solution of the differential equation for a generic time step t_{n+1} is [30]:

$$\boldsymbol{\varepsilon}_v \left(t_{n+1} \right) = \boldsymbol{\varepsilon}_v \left(t_n \right) + \frac{\Delta t}{\vartheta} \left[\boldsymbol{\varepsilon} \left(t_{n+1} \right) - \boldsymbol{\varepsilon}_v \left(t_n \right) \right] \tag{5}$$

The aforementioned viscous model is coupled with the well-known Tension-Compression Damage Model [31]. Such model is based on a split of the effective (elastic) stress tensor into tensile and compressive components, $\bar{\boldsymbol{\sigma}}^+$ and $\bar{\boldsymbol{\sigma}}^-$, according to the different mechanical behavior in tension and compression of the material:

$$\bar{\boldsymbol{\sigma}}^+ = \sum_{i=1}^{3} \left\langle \bar{\sigma}_i \right\rangle \mathbf{p}_i \otimes \mathbf{p}_i \quad \text{and} \quad \bar{\boldsymbol{\sigma}}^- = \bar{\boldsymbol{\sigma}} - \bar{\boldsymbol{\sigma}}^+ \tag{6}$$

The definition of two internal scalar damage variables d^+ and d^- under tension and compression respectively, ranging from 0 to 1 from an elastic to completely damaged material, leads to the constitutive model:

$$\boldsymbol{\sigma} = \left(1-d^+\right)\bar{\boldsymbol{\sigma}}^+ + \left(1-d^-\right)\bar{\boldsymbol{\sigma}}^- \tag{7}$$

This model entails directional orthotropic damage with dependence on principal directions of stress, i.e. the cracks arise according to different failure criteria and grow in different manners under tensile or compressive stress states [32]. The evolution of damage indexes $d^{\pm}$ is an exponential softening related to tensile and compressive fracture energies $G_f^{\pm}$ of the material, normalized according to the finite element characteristic length, in order to ensure objectivity of the FEM solution respect to the mesh size [33].

The coupling of the tension-compression damage model with the viscoelasticity model is carried out by assuming that the stress sustained by the Maxwell chain is the effective (undamaged) stress:

$$\bar{\boldsymbol{\sigma}} = \bar{\boldsymbol{\sigma}}_e + \bar{\boldsymbol{\sigma}}_v = \left(1-\xi\right)\mathbf{C}:\boldsymbol{\varepsilon} + \xi\mathbf{C}:\left(\boldsymbol{\varepsilon}-\boldsymbol{\varepsilon}_v\right) \tag{8}$$

The constitutive model accounting for the coupling between viscoelasticity and mechanical damage is eventually:

$$\boldsymbol{\sigma} = \left(1-d^+\right)\left(\bar{\boldsymbol{\sigma}}_e^+ + \bar{\boldsymbol{\sigma}}_v^+\right) + \left(1-d^-\right)\left(\bar{\boldsymbol{\sigma}}_e^- + \bar{\boldsymbol{\sigma}}_v^-\right) \tag{9}$$

The specific format of the model leads to several advantages especially in terms of simplicity and computational efficiency. The strain driven format, the reduced number of internal variables and input parameters are remarkable features of the model.

MODELLING OF CRACK LOCALIZATION

The tensile crack localization is modelled in the discrete problem by using a local crack-tracking technique [34,35]. This algorithm, implemented for 2D problems using three-node triangular elements, detects the finite element where a crack originates and then it allows the crack to develop as a function of the direction of the principal tensile stress along a single row of finite elements. The process is as follows. First, the crack origin is detected in elements that satisfy the tensile damage criterion. A crack-vector is drawn by using the direction perpendicular to the principal tensile direction of the element. The exit point is defined as the intersection of that vector with the corresponding face of the element. The entry point of the new element on the crack is located at the same coordinates of the exit point of the previous element. The next crack vector is drawn by using the direction perpendicular to the principal tensile direction of the new element. For each crack, the previous procedure is repeated until the whole crack path is defined. Discrete cracking is possible through the definition of a minimum distance between existing and new cracks. This distance is called as *exclusion radius* and is defined by the user, commonly considering the unit size of the masonry, as shown in [35]. The use of the tracking algorithm has shown to be capable of representing realistic results with clear collapse mechanisms induced by the development of discrete tensile cracks [35,36]. In addition, the numerical results are mesh-bias independent, i.e. they remain objective when different possible discretizations are considered in the FEM problem.

CASE STUDIES

Mallorca Cathedral

Mallorca Cathedral, with overall dimensions of 121 *m* in length and 55 *m* in width, is one of the most imposing Gothic buildings of the Mediterranean area. The central nave is 44 *m* high and 17.8 *m* wide, being one of the highest in the world. The lateral naves are 29 *m* high and 9 *m* wide. The piers have octagonal section with 1.5 ÷ 1.7 *m* circumscribed diameter and 22.7 *m* height. The slenderness ratio of the piers is around 14, i.e. much higher than the ratios usually encountered in French gothic churches, ranging between 7 and 9.

The cathedral underwent a long construction process lasting from 1306 to 1600, with long interruption periods (1460-1560). The building process was critical, bay after bay from the presbytery towards the façade, as usual in Gothic churches. The construction suffered partial collapses (e.g. the 4th vault from the apse partially collapsed 30 years after the construction), long periods between the construction of adjacent bays, and numerous repair interventions especially during the 18th and 19th centuries (e.g. dismantlement of Renaissance façade in 1851 due to 1.3 *m* out-of-plumb). The current condition of the cathedral is greatly characterized by the significant lateral deformation of the slender piers, with lateral displacements reaching even 1/90 of the height.

The 4th bay from the apse was investigated carefully by considering the historical records of the reconstruction process after its partial collapse (Figure 2), starting with chapels, followed by the piers, then the aisles and finally the central vault. During the last stage before the construction of the central vault, the piers were already receiving the in-ward thrust from the lateral naves, while the absence of the central one did not provide any counteracting action, thus creating a delicate stability condition. Such difficult equilibrium conditions during the construction

process, together with long-term time dependent phenomena and geometric nonlinearity, may have influenced the final deformation of the cathedral.

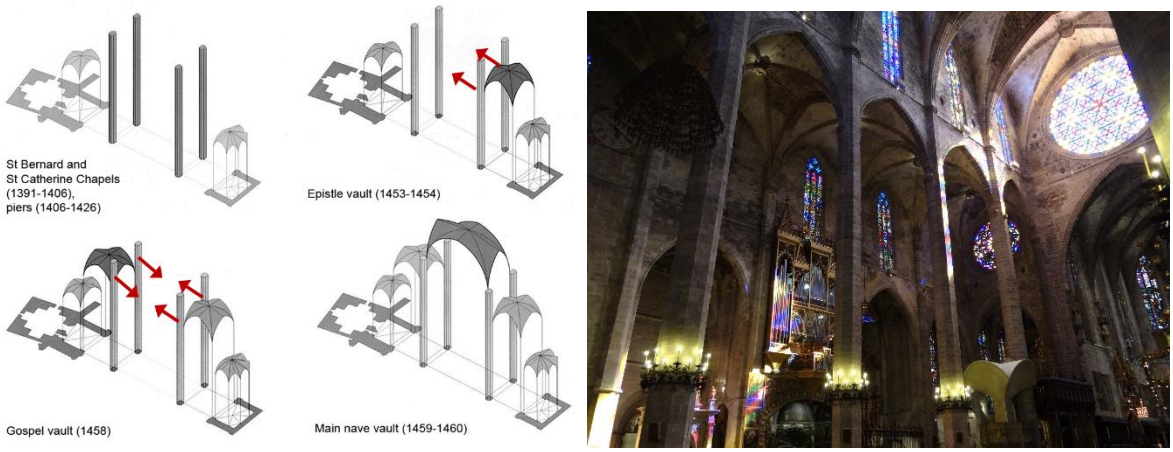

Figure 2: Construction process of the 4th bay of Mallorca Cathedral (left) [37,38], and view of the interior of the nave (right) [39].

The in-situ experimental activity allowed the quantification of the deformed condition of the cathedral. The lateral drift of the piers of the 4th bay was 95 *mm* with deformations increasing 0.1 *mm*/year (1 *cm*/century), as found in a continuous static monitoring survey developed between 2003 and 2008 [40]. The detected trend towards a progressive increase of deformation was of concern because, in combination with geometric nonlinear effects, it might worsen the stability conditions. For this reason, a FE simulation of the construction process of the representative bay was carried out to study the long-term behavior of the structure. This was possible through a staged analysis, considering the different construction phases and the long-term deformation simulated with the presented constitutive model. The available documents did not provide any clue on the utilization of provisional stabilizing devices, such as iron ties or timber struts, although their use is not totally disregarded [41].

Figure 3 presents the FEM model and Table 1 the material parameters adopted in the numerical simulations. FEM modelling considered one-fourth of the bay structure adopting adequate symmetrical conditions. The model is composed by 49,979 tetrahedral elements (14,689 nodes). The Young's modulus (E) and the specific weight (γ) for the different materials were defined making reference to the elastic calibration of the modelled structure reported in [42–44]. The values for the compressive strength (f_c) were estimated based on previous experience for similar masonry typologies in Spain. The tensile strength (f_t) was considered equal to 5% of the compressive one, while the values of the compressive and tensile fracture energies (Gf_c and Gf_t, respectively) were chosen based on previous experience.

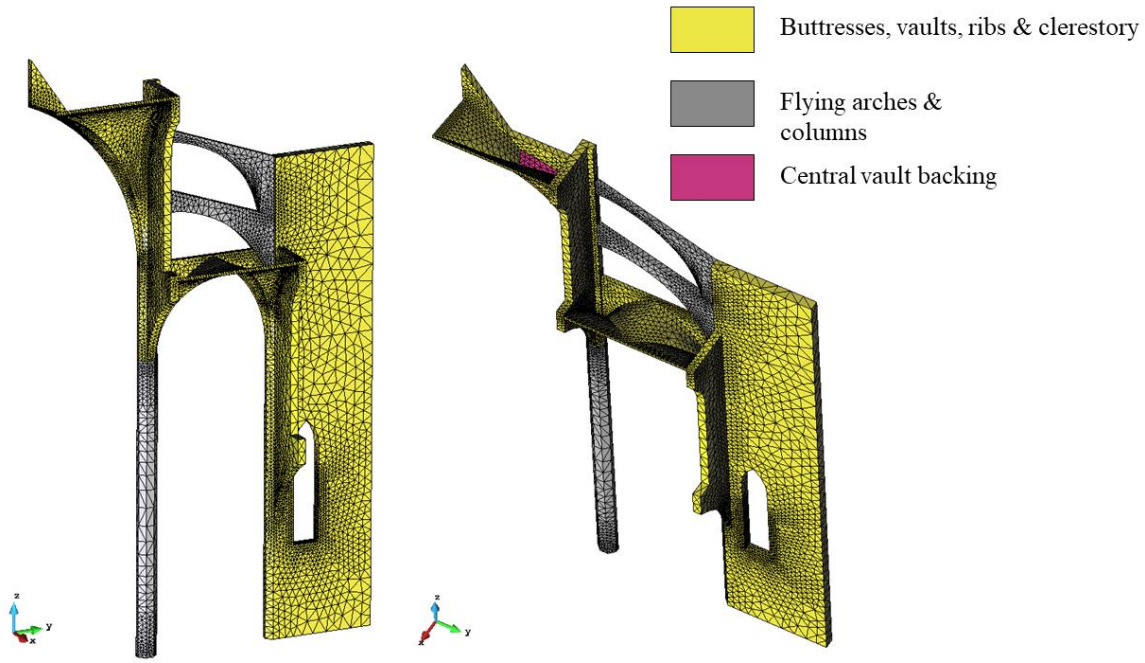

Figure 3: 3D finite element model of a quarter of a typical bay of Mallorca cathedral.

Table 1. Material properties used for the analysis of the Mallorca cathedral.

Element	f_c [MPa]	f_t [MPa]	E [MPa]	Gf_t [J/m^2]	Gf_c [J/m^2]	γ (kN/m^3)
Buttresses, vaults, ribs & clerestory	2.00	0.10	2000	100	40000	21.00
Flying arches & columns	8.00	0.40	8000	100	40000	24.00

Central vault backing	1.00	0.05	1000	100	40000	20.00

Thanks to a FE activation strategy able to reproduce the addition of different portions of the structure during the analysis, we could model sequentially the stages of the construction (Figures 4a-c). In particular, the FE activation strategy allows adding or removing parts of the FE mesh at selected stages of the analysis. In the first stage of the analysis of the studied bay, only the lower part of the FE model was activated, including the pier, the aisle vault and the buttress (Figure 4a) and analyzed under the effect of its self-weight. In the second stage, the upper part of the FE model was added to the existing one, including the upper part of the buttress, the flying arches, the clerestory and the nave vault (Figure 4b). Once the self-weight of the upper part was applied, the third stage of the analysis began. In this third stage, the structure was subject to constant loading due to its self-weight and the time started elapsing in order to evaluate the deformation accumulation due to creep (Figure 4c). The geometric nonlinearity was taken into account by adopting a total Lagrangian formulation with a small-strain/large-displacement assumption.

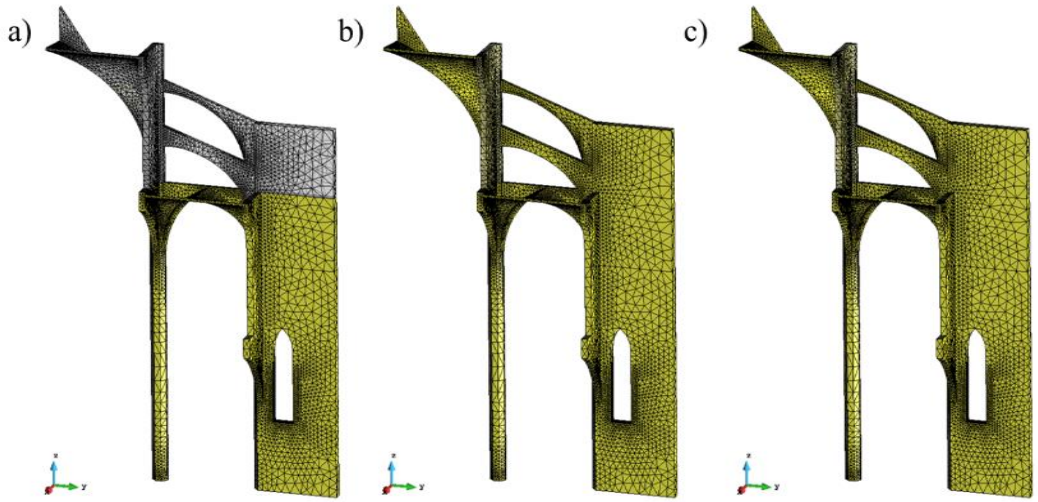

Figure 4: Staged analysis for the numerical simulation of the construction process of the 4th bay of Mallorca Cathedral: a) 1st stage considering as active the pier, the aisle vault and the lower part of the buttress, b) 2nd stage activating the upper part of the buttress, the flying arches, the clerestory and the nave vault, and c) study of the long-term response considering the whole structure.

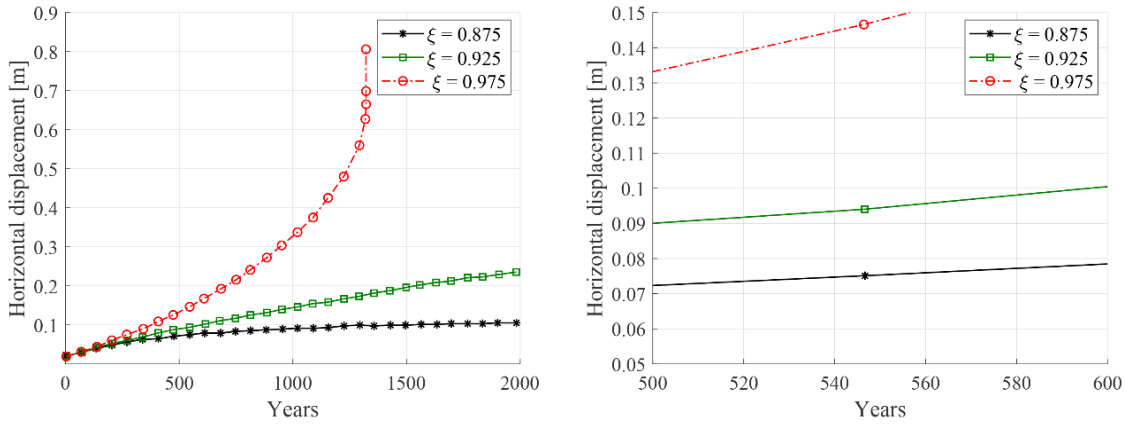

Figure 5: Time evolution of the horizontal displacement at the top of the pier for different values of the participation factor (left) and close up to the period between 500 and 600 years since the construction (right).

After the first construction phase (first stage of analysis), the resulting horizontal deformation at the top of the pier was equal to 30 *mm*. After the second construction phase (second stage of analysis), the maximum horizontal displacement at the pier decreased to 18 mm due to the application of the thrust of the central vault. The results of the third phase depend on two parameters of the viscous model, i.e. the retardation time and the participation ratio. These parameters were calibrated by a sensitivity analysis based on the experimental data derived from the monitoring activity. The calibration of the participation ratio showed that a value of 0.975 in the frame of a nonlinear geometric analysis leads to the instability of the structure at 1,350 years (Figure 5a). However, the most representative displacement vs. time curve is the one corresponding to a participation ratio of 0.925. For this participation ratio the numerical results agree with the data derived from the 2003-2008 monitoring period (lateral drift of the piers of 95 *mm* with deformations increasing 10 *mm*/century), corresponding to the years 543 and 548 after the completion of the structure (1460), see Figure 5b. A further monitoring period, now into consideration, would enable a more detailed estimation of the parameters involved. Notice

that a conventional instantaneous FEM analysis (i.e. without considering long-term deformation effects) would lead to a top displacement of only 7.6 *mm*.

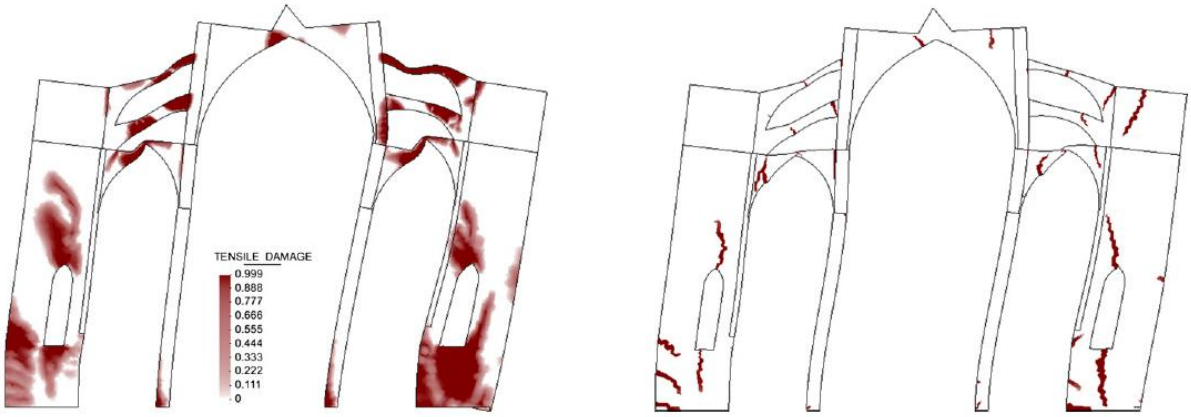

Figure 6: Collapse mechanism from pushover analysis with the smeared (left) and localized damage approach (right) [54].

The representative bay of Mallorca Cathedral was also analyzed under lateral horizontal forces by means of a pushover analysis, in order to evaluate the collapse condition under seismic actions and to illustrate the crack localization obtained through the use of the crack-tracking approach. Despite the limitation of not considering dynamic effects that may influence significantly the seismic response, pushover analysis is a conventional methodology [45,46] for studying the effect of seismic actions providing important information on the performance of the structure under the horizontal loading caused by seismic actions. The pushover analysis was performed in two stages: i) application of the self-weight and ii) application of a horizontal loading proportional to the mass.

The FEM model using the crack-tracking technique provides a realistic representation of the tensile cracks, allowing a clearer understanding of the collapse mechanism than in the traditional smeared crack approach (Figure 6). The more damaged portions of the bay are the base of columns and buttresses, as well as the aisle vaults and the flying buttresses. The damage is

minor in the nave vault, since the diaphragmatic transverse arch above the vault provides additional transversal stiffness.

Church of the Poblet Monastery

The monastery of Poblet, located in Catalonia (Spain) is a UNESCO World Heritage Site since 1991. The construction of the church of the complex started in 1170 and was completed in 1276. The church is a typical example of Cistercian architecture, characterized by both Romanesque (barrel vault) and Gothic styles (pointed arches and pointed groin vaults). The east part of the church is composed by the apse, the ambulatory and its five radiating chapels, while the west one by three naves. The transept makes the transition between the two parts and gives the church a Latin cross shape plan. A pointed barrel vault with a series of arches aligned with the lateral piers covers the main nave. The vaulting in the lateral aisles is distinct. The northern aisle follows the original design with pointed groin vaults, while the southern one follows a Gothic style and is the result of a demolition and reconstruction of the 14th century. Due to this intervention, the structure is asymmetrical in the transverse direction. Notably, a similar intervention occurred in Fontfroide (France), and the motivation behind those were probably to host lateral chapels for noble and wealthy families. Figure 7 presents the main and the two lateral naves of the church.

Figure 7: Southern (left), main (middle) and northern (right) naves of the church of the Poblet monastery.

The church presents damage today mostly at its western part. A laser-scanner survey has shown that the barrel vault presents a deflection of 500 *mm* and the clerestory walls have outwards deformations of 140 *mm* in the southern side and 100 *mm* in the northern side. Important cracking is evident in the barrel vault near its key, continuing longitudinally across almost all the bays of the church. Local stone crushing is visible at the middle height of the arches in the main nave. In the lateral aisles, longitudinal cracks are evident near the key of the vaults, accompanied by relative vertical displacements of 50 ÷ 70 *mm*.

The structural analysis aimed at identifying the causes of the existing damage at the west part of the church. The construction of the main and lateral naves as a sequence of identical bays and the damage pattern, which is similar for all the bays, allows the simulation of only a bay of the church considering the necessary symmetry conditions. The FEM model was prepared considering the real deformed geometry of the fourth bay structure, presenting the highest deflection of the barrel vault. This choice aims to take into account the influence of the existing deformation on the stability of the structure. The geometry was available through a terrestrial laser-scanning survey. The final model (shown in Figure 8) is composed by 291,101 tetrahedral

elements (61,438 nodes) and includes three different materials: squared stone masonry, infill of the barrel vault and infill of the three-leaf walls and vaults. The material properties, shown in Table 2, were defined based on existing studies of the church [47,48], as well as on the recommendations of technical standards [49,50]. "Masonry" in Table 2 corresponds to the square stone limestone masonry of the external leaves of the pillars, walls and vaults of the structure. The chosen values for the compressive strength and the Young's modulus correspond to the lower bounds proposed for square stone masonry in [50]. The corresponding properties for the rest of the materials were defined following the in-situ investigation of the structure and a sensitivity analysis reported in [51]. As for the case of the Mallorca cathedral, the tensile strength was considered as 5% of the compressive one, while the tensile and compressive fracture energies have been defined based on the experience of the authors from the modelling of similar structures. Note, that the issue of the high uncertainty in the material properties is very important and for this is assessed in the following section of this work.

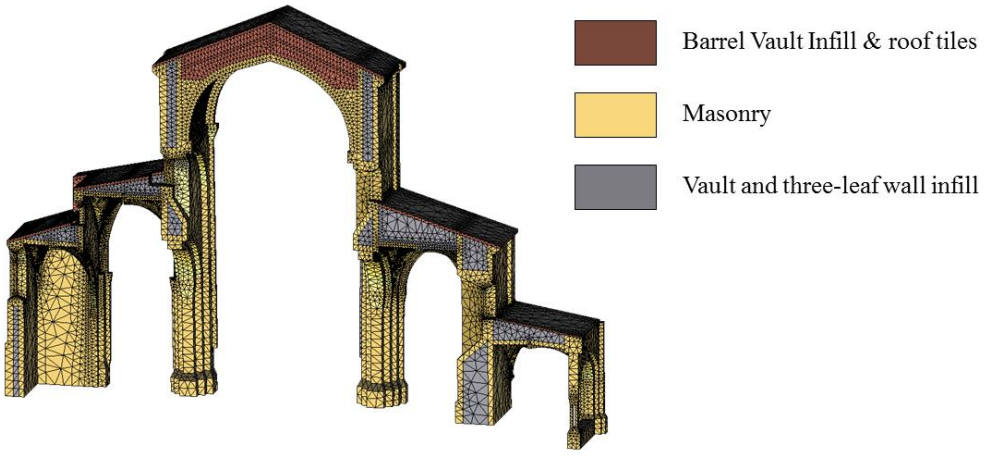

Figure 8: 3D finite element model of the 4th bay of the church of the Poblet Monastery.

Table 2: Material properties used for the analysis of the church of the Poblet monastery.

Element	f_c [MPa]	f_t [MPa]	E [MPa]	Gf_t [J/m^2]	Gf_c [J/m^2]	γ (kN/m^3)
Masonry	6.0	0.300	2400	150	40000	22.00
Vault and three-leaf wall infill	1.5	0.075	800	20	4000	19.00
Barrel vault infill & roof tiles	0.5	0.025	25	20	4000	18.00

The structural analysis strategy was based on the results of an in-situ inspection and a historical investigation and included three analysis scenarios that could potentially produce the current pathology: gravitational loads, past structural alterations, seismic actions.

The first structural analysis scenario investigates the current condition of the structure under only gravitational loading. This numerical simulation predicts damage in good agreement with the existing in the structure (Figure 9). At the end of the analysis, cracks exist near the key of the barrel vault, as well as at the top of the lateral vaults. These results show that the current geometrical configuration of the bay justifies the existence of cracks in the vaults.

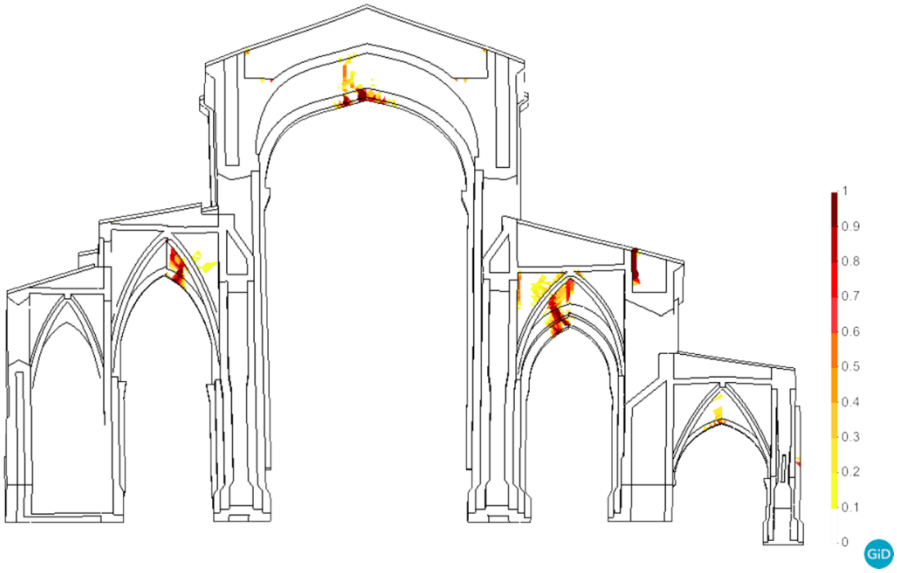

Figure 9: Contour of the tensile damage under the effect of gravitational load.

The second structural analysis simulates a procedure that was possibly followed for the demolition and reconstruction of the southern lateral nave during the intervention of the 14th

century. According to this, each bay of the lateral nave was demolished and reconstructed before proceeding to the following one. This scenario was simulated in two stages through a staged analysis that allowed activating and deactivating parts of the finite element mesh during the analysis. In the first stage, the gravitational load was applied to the whole structure, while in the second one the demolition of the lateral nave was simulated by deactivating (i.e. removing) the finite elements corresponding to it (shown in green in Figure 10a). For this analysis, the numerical model includes one bay of the southern half of the church and two adjacent bay quarters at each side (347,626 tetrahedral elements and 76,399 nodes). The numerical simulation of the demolition of the lateral aisle causes a higher rotation of the southern clerestory wall and a higher deflection in the barrel vault with an important increase of 430% and 30%, respectively, comparing to the initial state. These results may explain the asymmetric drift of clerestory walls (larger at south) that potentially increased the deflection of the central vault and initiated or extended the damage at its top (Figure 10b).

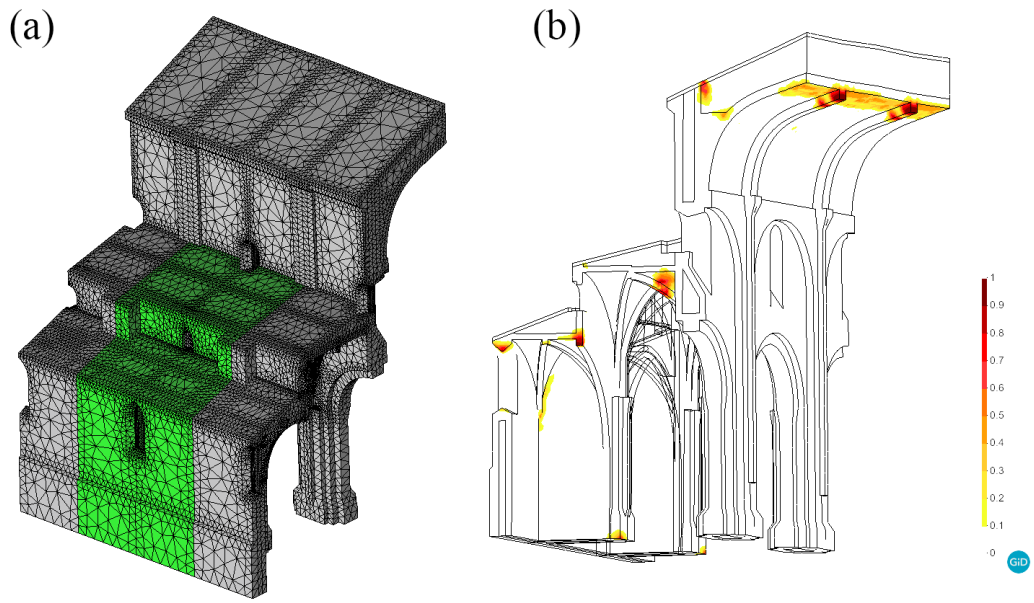

Figure 10: (a) Model used for the simulation of the demolition of the lateral nave (mesh in green colour) and (b) contour of the tensile damage at the end of the simulation.

The possible effect of a past earthquake (occurred in 1792) in the structure was also assessed through pushover analysis. Due to the asymmetrical geometrical configuration of the lateral naves, two analyses were performed considering the two directions transversal to the longitudinal axis of the main nave. The analyses show that the cracking in the main and lateral naves could have been further extended due to an earthquake (Figure 11). Interestingly, the numerical analyses predict a high accumulation of compressive stresses at the intrados of the arches in the main and lateral naves, where local stone crushing is observed today at the church (Figure 12). The seismic analysis indicates that an earthquake could have initiated or extended the wide cracking near the key of the barrel vault, producing at the same time crushing of the stone in the arches of the main and lateral aisles.

Figure 11: Contour of the tensile damage for the pushover analysis towards south (top) and north (bottom).

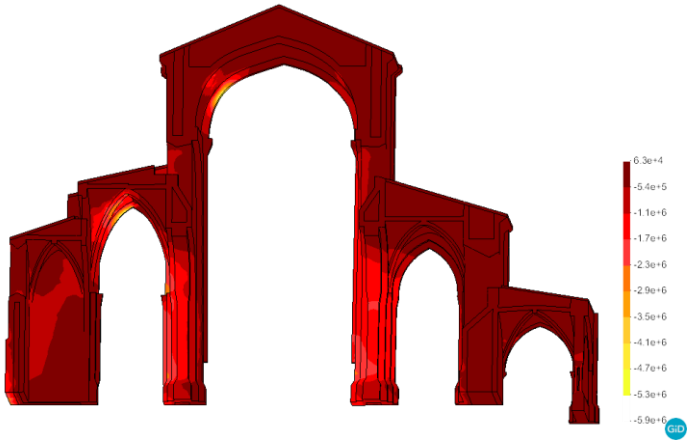

Figure 12: Contour of the compressive stresses at the end of the pushover analysis towards the south direction. Compressive stress accumulation at the interior of the arches in the main and lateral nave.

The various structural analysis cases could shed light on the possible causes for the existing damage and deformation of the west part of the church. The initial design of the church, with the two lateral naves being much lower than the central one, seems to be sufficient to produce cracking near the keys of the main and lateral naves. This height difference may have produced the spreading of the springs of the barrel vault and thus the rotation of the south and north piers of the main nave. The demolition of the southern nave during the intervention of the 14th century could have produced the higher rotation of the southern pier as observed today. Finally, the local crushing appearing in the arches of the main and lateral naves could be the result of past seismic actions affecting the region.

SEISMIC ASSESSMENT CONSIDERING UNCERTAINTY OF MATERIAL PROPERTIES AND NUMERICAL PARAMETERS

Numerical modelling of masonry structures requires the a priori definition of the mechanical properties and numerical parameters, the number and type of which is specified by the

adopted constitutive model and the numerical strategy. Some of the material properties can be obtained through standardized experimental testing (e.g. compressive strength, Young's modulus), while others are more difficult to obtain and the available experimental evidence is limited (e.g. tensile strength, fracture energy). In most cases, the cultural value of monuments impedes an extensive experimental investigation that could provide values for the material properties used by the constitutive models. Even in the case where in-situ (through non- or minor-destructive techniques) or laboratory testing of extracted probes is possible, the results may present important variation. This uncertainty related to the material properties is usually neglected in the numerical modelling of historical structures, and the material properties are defined either in a deterministic way, by considering the average values of available experimental results, or artificially, based on experimental databases included in technical standards.

Another source of uncertainties in the numerical analyses is given by the necessary numerical parameters. For instance, the crack-tracking algorithm, presented in a previous section, uses the *exclusion radius* that is a parameter defining the distance between distinct cracks in the FEM model. As shown in previous studies [35,52], this numerical parameter can be selected according to the dimensions of the units in the investigated masonry, considering in an implicit way the staggering pattern of the investigated masonry. Nevertheless, large complex structures as the ones investigated in this work, are usually composed by different unit sizes, as well as different masonry typologies within the same fabric (e.g three-leaf walls, irregular stone masonry, etc.). For this, the use of a single deterministic value may not be representative, and different cases should be investigated.

Despite the existence of these uncertainties, most of the numerical analyses of historical structures in the available literature are based on the use of deterministic models. On the one hand, geometry plays a very important role in the stability and the identification of the collapse

mechanisms of masonry structures. This is why numerical studies using deterministic values can be helpful in identifying the causes of existing pathology and the stability of a masonry structure, as shown in the previous sections. On the other hand, the above uncertainties in material properties and numerical parameters become important when the objective of the structural analysis is to draw conclusions over the capacity and safety under any investigated scenario. To achieve this objective, the structural analysis should follow a probabilistic methodology considering the sources of uncertainty in the analyzed structure. This section presents the application of such a methodology for the assessment of the seismic vulnerability of a representative bay of the Poblet monastery.

Probabilistic analysis of the seismic vulnerability of the church of Poblet monastery

The seismic assessment of a representative bay of the church of the Poblet monastery is carried-out in this section using a Monte Carlo-type simulation based on a Latin Hypercube Sampling. The aim of the analysis is to derive fragility curves representing the seismic vulnerability of the investigated structure for three different levels of damage.

Random variables

The first step in the probabilistic analysis is the definition of the random variables. Here we consider the uncertainty of six random variables. Five of them are material properties, while the sixth is a numerical property used in the crack-tracking algorithm. As uncertain material properties we consider the compressive strength and the Young's modulus of the masonry (f_c^{mas}, E^{mas}) and of the infill of the lateral vaults (f_c^{inf}, E^{inf}). The last material random variable is the tensile strength of the two materials, which is considered as a fraction of the compressive one (f_t / f_c). The stochastic characterization of these five random variables (f_c^{mas}, E^{mas}, f_c^{inf}, E^{inf}, f_t/f_c) is through the use of lognormal probability distributions. The value of the mean (μ) and standard

deviation of the logarithm (σ_{ln}) are presented in Table 3. The mean values are the same to the ones used for the 3D model, presented in the preceding section, apart from the Young's modulus of masonry, which is slightly lower. This is due to the fact that three-leaf masonry is considered as a homogenous material with average properties in the numerical model used in the probabilistic analysis. The value of 2100 MPa is the result of a calibration procedure, detailed in the following section. The values for σ_{ln} are selected based on the recommendations of [46]. In particular, the standard deviations of the infill of the vaults and of the masonry are defined considering values corresponding to those of an irregular stone masonry and of a three-leaf wall, respectively. The tensile strength is usually defined in the literature as a fraction of the compressive strength, which varies between 0.03 and 0.10 [53–55]. Due to this, f_t / f_c is simulated in this work as a random variable, assuming a similar variation with that of the compressive strength of the infill of the vaults by adopting a lognormal distribution with a mean value of 6.5% and a standard deviation of 0.29. The material properties of the infill of the barrel vault are deterministically defined as equal to those used in the 3D model. This is due to our knowledge of these material properties following an in-situ investigation and their limited influence in the structural capacity of the church [56].

As already stated, the exclusion radius (r_{excl}) defines the distance between discrete cracks in the FEM model and its value is related to the size of the units in the investigated masonry [35,52]. Despite the association of the exclusion radius with a material characteristic (i.e. the unit size), it is a numerical parameter characterized by epistemic uncertainty. In this work, we consider it as a random variable following a uniform distribution. The two limits of the uniform distribution are equal to the two extreme lengths of the stone units found in the investigated church, i.e. 0.10 and 1.10 m [56].

Table 3: Values of the mean and standard deviation of the logarithm for the five material random variables

	f_c^{mas} [MPa]	E^{mas} [MPa]	f_c^{inf} [MPa]	E^{inf} [MPa]	f_t/f_c [%]
μ	6.0	2100	1.5	800	6.5
σ_{ln}	0.20	0.17	0.29	0.21	0.29

Sampling procedure

The effect of the presented random variables on the seismic response of the investigated masonry structure is evaluated using stochastic simulation. Here, we generate and analyze *N=200* combinations of random samples of the uncertain parameters through a Monte Carlo-type simulation. For the sampling procedure, we use a Latin Hypercube Sampling, aiming to reduce the variance of standard Monte Carlo Simulation and, thus, use less samples. The number of samples (*N=200*) is selected based on previous experience of the authors with similar structures [57]. Figure 13 presents the sampling for the six random variables.

Due to the large number of analyses, an efficient numerical strategy is necessary to guarantee the application of the methodology. For this, all the analyses are performed with a 2D plane stress finite element model of the investigated structure. This 2D model represents the 4th bay of the west part of the church Poblet monastery, as the 3D one used in the preceding section. The 2D model was calibrated so that it presents an equivalent response in terms of stiffness and capacity both under gravitational and horizontal in-plane loading, as well as in terms of modal shapes and frequencies under modal analysis. Figure 14 shows the used 2D model, which is composed by 25578 constant strain 3-node triangles (13425 nodes).

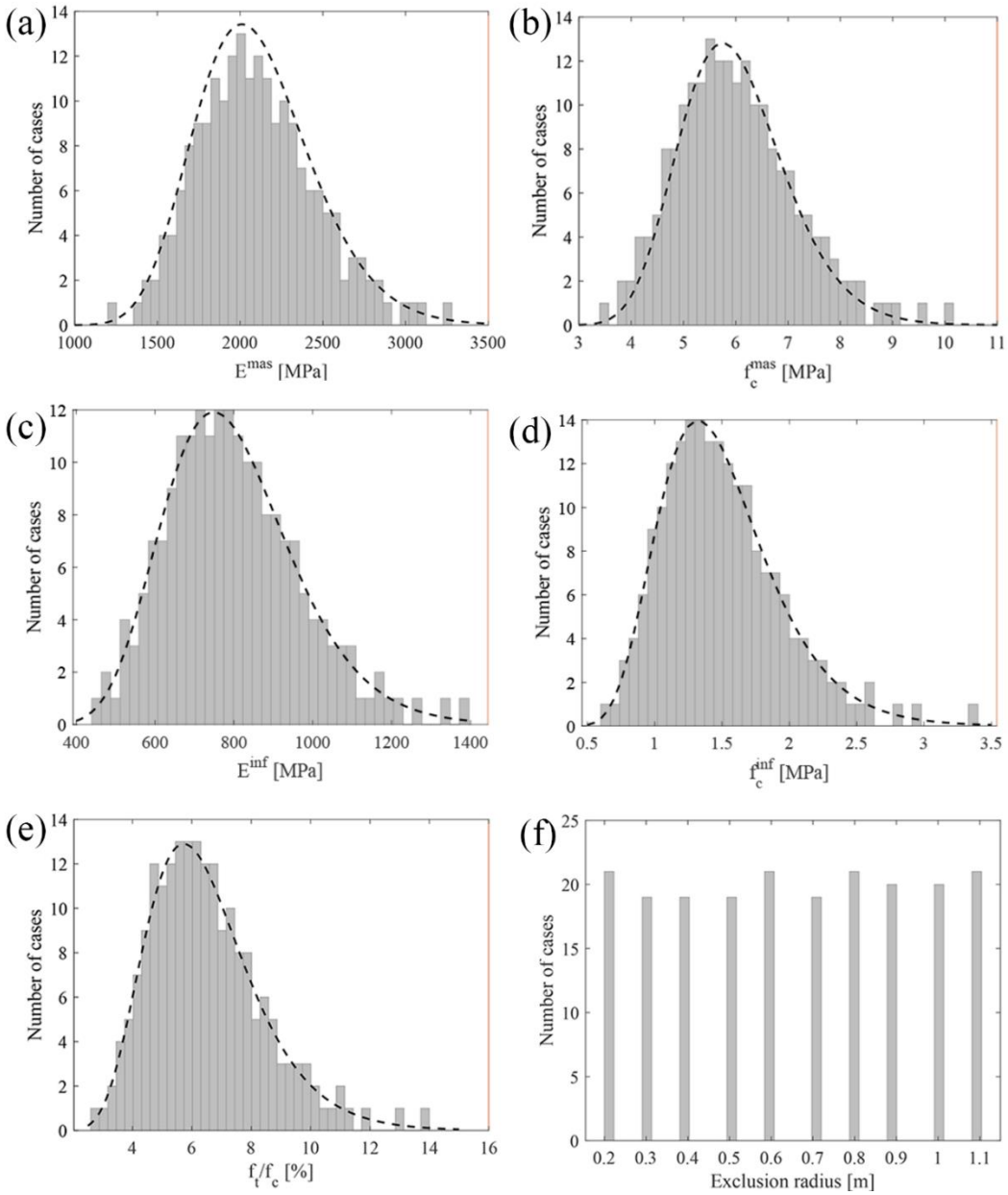

Figure 13: Histograms with the distributions of the sampled values and corresponding lognormal probability density functions (in dashed line) for (a) f_c^{mas}, (b) E^{mas}, (c) f_c^{inf}, (d) E^{inf}, (e) f_t/f_c, and uniform distribution for (f) Exclusion radius.

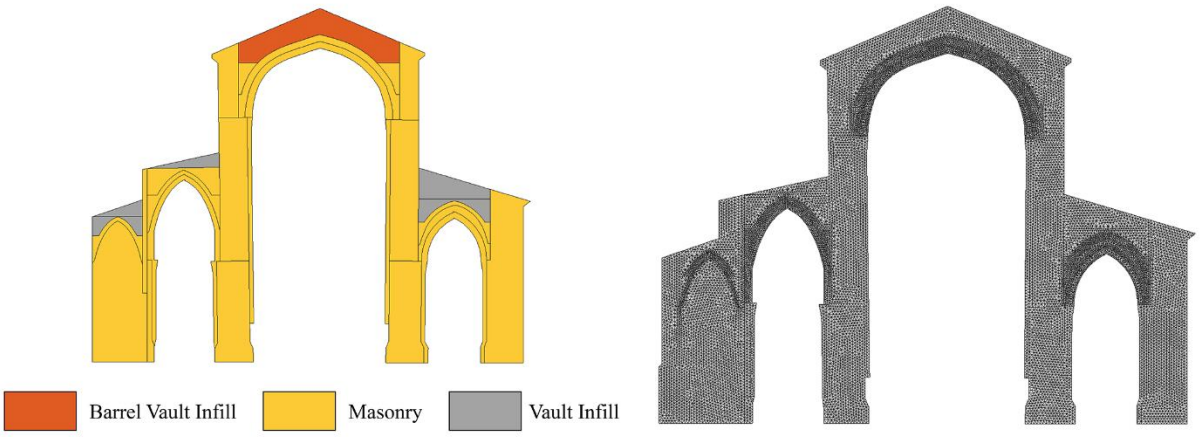

Figure 14: Material distribution (left) and finite element mesh (right) of the plane stress finite element model of the 4th bay of the church of Poblet monastery used in the probabilistic seismic assessment.

The seismic behavior of the structure is evaluated through pushover analysis with a force distribution proportional to the mass towards the north direction, which was identified as the most vulnerable case. Figure 15 presents the capacity curves (horizontal acceleration vs. horizontal displacement at the top of the nave) for the 200 analyzed cases. The variation of the material and numerical properties results to a horizontal capacity ranging between 0.05 *g* and 0.16 *g*.

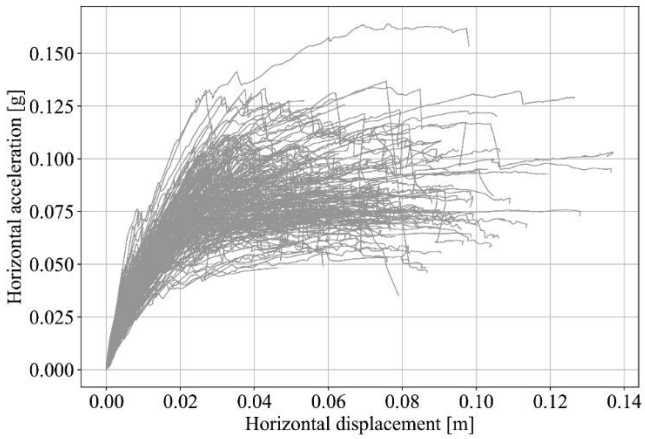

Figure 15. Capacity curves for the 200 analyzed cases

Limit states

Figure 16 illustrates a generic capacity curve of the church for one of the studied cases. In the capacity curve it is possible to identify three different parts. Each of them corresponds to a different limit state caused by the onset and propagation of cracks in the main and lateral naves. The first limit state LS1 corresponds to a 15% drop in the lateral stiffness and it is shown with a green dot in Figure 16. This drop occurs due to the propagation of cracking in the barrel vault of the main nave (see Figure 17a). The second limit state LS2 corresponds to the maximum capacity and the initiation of the post-peak branch. For most of the analyzed cases, as the one with the capacity curve shown in Figure 16, LS2 corresponds to the local crushing of the stone in the barrel vault of the main nave, shown with a green circle in Figure 17b. The last limit state LS3 corresponds to the displacement level at the top of the barrel vault for which a drop of 20% of the lateral capacity occurs. For the analyzed case of Figures 16 and 17, this occurs due to the local crushing of the stone at the northern lateral vault (see green circle in Figure 17c).

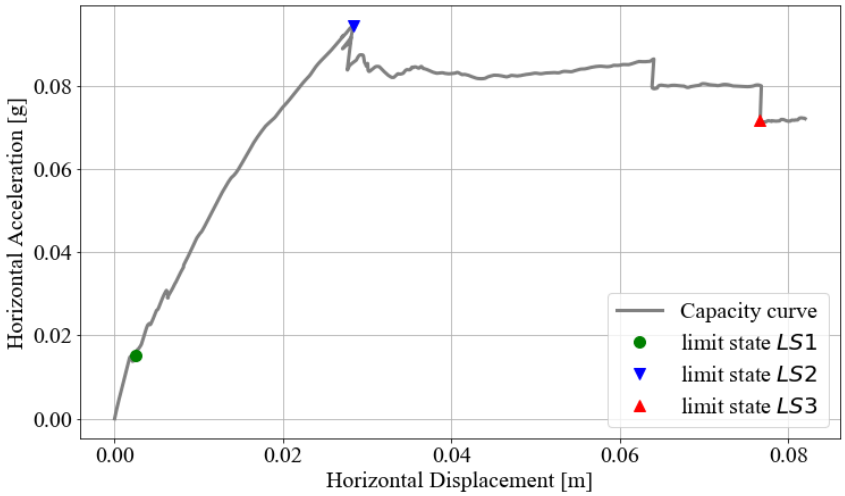

Figure 16: Capacity curve of one analyzed cases and the corresponding three limit states.

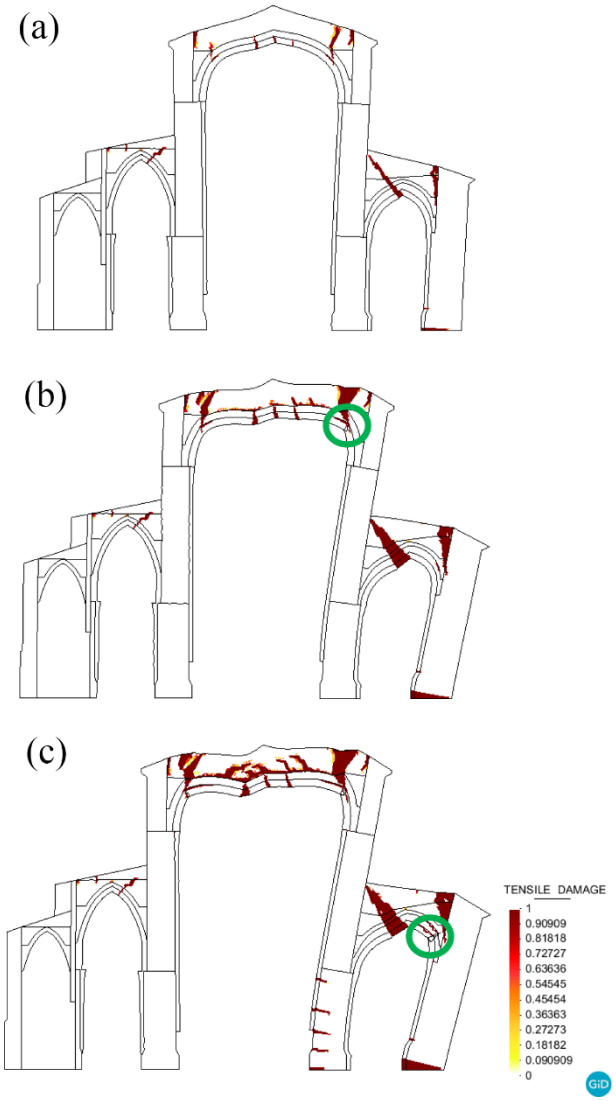

Figure 17: Tensile damage contour in a studied case corresponding to Limit State 1 (top), Limit State 2 (middle) and Limit State 3 (bottom).

Fragility curves

Figure 18 plots the fragility curves in function of the peak ground acceleration (PGA). The PGA corresponding to each limit state was computed following the N2 method as defined in [58] and included in national and international codes [45,59]. The fragility functions are defined according to [60] as

$$P[LS_i|PGA] = \Phi\left[\frac{1}{\beta_{LS_i}} ln\left(\frac{PGA}{\theta_{LS_i}}\right)\right]. \quad (10)$$

where β_{LS_i} is the standard deviation of the natural logarithm of the PGA for limit state LS_i, θ_{LS_i} is the median value of the PGA at which the analysed structure reaches the limit state LS_i, and Φ is the standard normal cumulative distribution function. θ_{LS_i} and β_{LS_i} are computed through the following functions

$$\theta_{LS_i} = e^{\left(\frac{1}{N}\sum_{j=1}^{N} \ln PGA_j\right)} \approx PGA_{50\%} \quad (2)$$

$$\beta_{LS_i} = \sqrt{\frac{1}{N-1}\sum_{j=1}^{N}\left(ln\left(\frac{PGA_j}{\theta_{LS_i}}\right)\right)^2} \quad (3)$$

where N=200 is the selected number of structural samples analysed in the Monte Carlo-type stochastic simulation and PGA_j is the Peak Ground Acceleration for the analysed case $j = 1, N$. This lognormal definition of the fragility functions fits very well the cumulative fragility functions for all the limits states, shown in red in Figure 18.

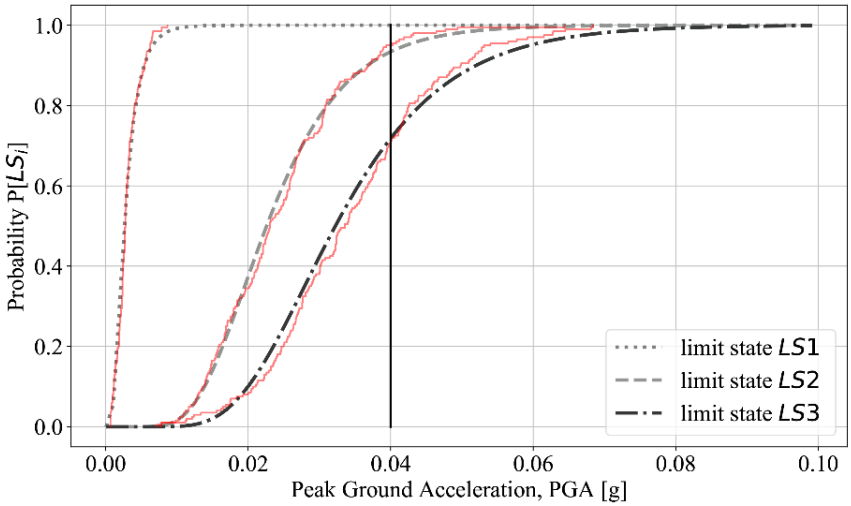

Figure 18: Fragility curves for the three limit states (LS1-LS3) in terms of Peak Ground Acceleration (PGA). The vertical line corresponds to PGA = 0.04g, i.e. the seismic demand for the region of L'Espluga de Francoli with a 500-year return period.

The results show that earthquakes with very low intensity are sufficient to produce a damage in the structure resulting in a 15% drop of the original stiffness (i.e. Limit State 1). In fact, there is an almost 100% probability for LS1 to occur for a PGA = 0.04g, which corresponds to the seismic acceleration demand for the region of L'Espluga de Francoli where the monastery is located for a return period of 500 years. For the same seismic demand, the probability of LS2 and LS3 is 92.5% and 69.7% respectively. This high probability of damage even for low seismic intensities can be attributed to the original design of the church, with important mass at the barrel vault of the main nave lacking of buttressing and the low height of the lateral naves.

CONCLUSIONS

The protection and conservation of built cultural heritage is a challenging task relying on the implementation of a multidisciplinary scientific approach based on inspection, structural analysis and monitoring. The aforementioned stages of the scientific approach are part of a cyclic procedure within which the results of each stage are used to update the rest, helping in taking informative decisions regarding the conservation strategy. Structural analysis has an important role within this procedure, as it can aid to understand the causes of the structural pathology and its evolution as identified by inspection and monitoring activities, respectively. In addition, it can guide the design of an intervention and investigate its structural efficiency.

Today, structural analysis of complex historical masonry structures is largely based on the use of advanced computational tools. This structural analysis approach faces the challenge to properly calibrate and validate the numerical models against empirical evidence on damage affecting the structure. This paper presented the use of numerical tools for structural analysis and their combination with historical investigation, in-situ inspection and monitoring activities for two important large masonry historical structures in Spain, i.e. the Mallorca Cathedral and

the church of the Poblet Monastery. A numerical strategy based on the use of a macromodelling approach was chosen as a way to reduce the computational cost and to permit the efficient analysis of the large-scale structures. Important role in this strategy plays the constitutive model, which was chosen to properly represent the distinct nonlinear tensile and compressive behaviour of masonry, as well as its time-dependent response. The application of this methodology to two case studies permitted the interpretation of their current pathology and allowed to take optimum decisions of future studies, such as the definition of monitoring activities.

Structural analysis of complex historical structures are usually influenced by important uncertainties related with the material properties and the numerical parameters of the adopted computational tool. To address these challenges, a probabilistic methodology was applied for the seismic assessment of the church of the Poblet monastery. A Monte-Carlo type simulation was carried out considering five material properties and one numerical parameter as random variables. A total number of 200 structural models with different combinations of the random variables were prepared and analyzed against horizontal seismic loading (pushover analysis). The results of the analyses were used to derive fragility curves for three limit states corresponding to different levels of damage in the structure. The results showed that the structure presents a high vulnerability for the seismic demand of the area of L'Espluga de Francolí.

ACKNOWLEDGEMENTS

The authors would like to thank the Ministry of Science, Innovation and Universities (MCIU) of the Spanish Government, the State Agency of Research (AEI) and the European Regional Development Fund (ERDF) through the SEVERUS project (Multilevel evaluation of seismic vulnerability and risk mitigation of masonry buildings in resilient historical urban centres ref. num. RTI2018-099589-BI00).

DATA AVAILABILITY

Some or all data, models, or code that support the findings of this study are available from the corresponding author upon reasonable request.

REFERENCES

[1] ICOMOS/ISCARSAH. Recommendations for the analysis, conservation and structural restoration of architectural heritage. See Www Icomos Org 2005:1–38.

[2] ISO/TC98. ISO/FDIS 13822: Bases for design of structures-Assessment of existing structures 2010.

[3] Taliercio A, Binda L. The Basilica of San Vitale in Ravenna: Investigation on the current structural faults and their mid-term evolution. J Cult Herit 2007;8:99–118. doi:10.1016/j.culher.2006.09.005.

[4] Milani G, Valente M. Comparative pushover and limit analyses on seven masonry churches damaged by the 2012 Emilia-Romagna (Italy) seismic events: Possibilities of non-linear finite elements compared with pre-assigned failure mechanisms. Eng Fail Anal 2015;47:129–61. doi:10.1016/j.engfailanal.2014.09.016.

[5] Lourenço PB, Trujillo A, Mendes N, Ramos LF. Seismic performance of the St. George of the Latins church: Lessons learned from studying masonry ruins. Eng Struct 2012;40:501–18. doi:10.1016/j.engstruct.2012.03.003.

[6] Ortega J, Vasconcelos G, Rodrigues H, Correia M. Assessment of the influence of horizontal diaphragms on the seismic performance of vernacular buildings. Bull Earthq Eng 2018. doi:10.1007/s10518-018-0318-8.

[7] Betti M, Borghini A, Boschi S, Ciavattone A, Betti M, Borghini A, et al. Comparative Seismic Risk Assessment of Basilica- type Churches. J Earthq Eng 2017;00:1–34.

doi:10.1080/13632469.2017.1309602.

[8] Compán V, Pachón P, Cámara M, Lourenço PB, Sáez A. Structural safety assessment of geometrically complex masonry vaults by non-linear analysis. The Chapel of the Würzburg Residence (Germany). Eng Struct 2017;140:1–13. doi:10.1016/j.engstruct.2017.03.002.

[9] Milani G, Shehu R, Valente M. Seismic Assessment of Masonry Towers by Means of Nonlinear Static Procedures. Procedia Eng 2017;199:266–71. doi:10.1016/j.proeng.2017.09.022.

[10] Lasciarrea WG, Amorosi A, Boldini D, de Felice G, Malena M. Jointed Masonry Model: A constitutive law for 3D soil-structure interaction analysis. Eng Struct 2019;201:109803. doi:10.1016/j.engstruct.2019.109803.

[11] Iannuzzo A, Angelillo M, De Chiara E, De Guglielmo F, De Serio F, Ribera F, et al. Modelling the cracks produced by settlements in masonry structures. Meccanica 2018;53:1857–73. doi:10.1007/s11012-017-0721-2.

[12] Drougkas A, Verstrynge E, Szekér P, Heirman G, Bejarano-Urrego LE, Giardina G, et al. Numerical Modeling of a Church Nave Wall Subjected to Differential Settlements: Soil-Structure Interaction, Time-Dependence and Sensitivity Analysis. Int J Archit Herit 2019. doi:10.1080/15583058.2019.1602682.

[13] Giardina G, van de Graaf A V., Hendriks MAN, Rots JG, Marini A. Numerical analysis of a masonry façade subject to tunnelling-induced settlements. Eng Struct 2013;54:234–47. doi:10.1016/j.engstruct.2013.03.055.

[14] Papa E, Taliercio A. A visco-damage model for brittle materials under monotonic and sustained stresses. Int J Numer Anal Methods Geomech 2005;29:287–310. doi:10.1002/nag.415.

[15] Verstrynge E, Schueremans L, Van Gemert D, Hendriks MAN. Modelling and analysis of time-dependent behaviour of historical masonry under high stress levels. Eng Struct 2011;33:210–7. doi:10.1016/j.engstruct.2010.10.010.

[16] Cecchi A, Tralli A. A homogenized viscoelastic model for masonry structures. Int J Solids Struct 2012;49:1485–96. doi:10.1016/j.ijsolstr.2012.02.034.

[17] Roca P, Cervera M, Gariup G, Pelà L. Structural Analysis of Masonry Historical Constructions. Classical and Advanced Approaches. Arch Comput Methods Eng 2010;17:299–325. doi:10.1007/s11831-010-9046-1.

[18] Theodossopoulos D, Sinha B. A review of analytical methods in the current design processes and assessment of performance of masonry structures. Constr Build Mater 2013;41:990–1001. doi:10.1016/j.conbuildmat.2012.07.095.

[19] D'Altri AM, Sarhosis V, Milani G, Rots J, Cattari S, Lagomarsino S, et al. Modeling Strategies for the Computational Analysis of Unreinforced Masonry Structures: Review and Classification. Springer Netherlands; 2019. doi:10.1007/s11831-019-09351-x.

[20] Gambarotta L, Lagomarsino S. Damage models for the seismic response of brick masonry shear walls. Part I: The mortar joint model and its applications. Earthq Eng Struct Dyn 1997;26:423–39. doi:10.1002/(SICI)1096-9845(199704)26:4<423::AID-EQE650>3.0.CO;2-#.

[21] Macorini L, Izzuddin BA. A non-linear interface element for 3D mesoscale analysis of brick-masonry structures. Int J Numer Methods Eng 2011;85:1584–608. doi:10.1002/nme.3046.

[22] Milani G, Venturini G. Safety Assessment of Four Masonry Churches by a Plate and Shell FE Non-Linear Approach. J Perform Constr Facil 2011:230. doi:10.1061/(ASCE)CF.1943-5509.0000321.

[23] Lourenço PB, Rots JG, Blaauwendraad J. Continuum Model for Masonry: Parameter Estimation and Validation. J Struct Eng 1998;124:642–52. doi:10.1061/(ASCE)0733-9445(1998)124:6(642).

[24] Gambarotta L, Lagomarsino S. Damage Models for the Seismic Response of Brick Masonry Shear Walls. Part II: the Continuum Model and Its Applications. Earthq Engng Struct Dyn 1997;26:441–62. doi:10.1002/(sici)1096-9845(199704)26:4%3C441::aid-eqe651%3E3.0.co;2-0.

[25] Papa E. A unilateral damage model for masonry based on a homogenisation procedure. Mech Cohesive-Frictional Mater 1996;1:349–66.

[26] Addessi D, Marfia S, Sacco E, Toti J. Modeling Approaches for Masonry Structures. Open Civ Eng J 2014;8:288–300.

[27] Binda L, Anzani A, Saisi A. Failures due to long-term behaviour of heavy structures: The Pavia Civic Tower and the Noto Cathedral. Adv. Archit., 2003.

[28] Brandonisio G, Lucibello G, Mele E, Luca A De. Damage and performance evaluation of masonry churches in the 2009 L'Aquila earthquake. Eng Fail Anal 2013;34:693–714. doi:10.1016/j.engfailanal.2013.01.021.

[29] Valente M, Barbieri G, Biolzi L. Damage assessment of three medieval churches after the 2012 Emilia earthquake. Bull Earthq Eng 2017;15:2939–80. doi:10.1007/s10518-016-0073-7.

[30] Roca P. Viscoelasticity and Damage Model for Creep Behavior of Historical Masonry Structures. Open Civ Eng J 2012;6:188–99. doi:10.2174/1874149501206010188.

[31] Faria R, Oliver J, Cervera M. A strain-based plastic viscous-damage model for massive concrete structures. Int J Solids Struct 1998;35:1533–58. doi:10.1016/S0020-7683(97)00119-4.

[32] Pelà L. Continuum Damage Model for Nonlinear Analysis of Masonry Structures. Universitat Politècnica de Catalunya (UPC-BarcelonaTech), 2009.

[33] Cervera M. Viscoelasticity and Rate-dependent Continuum Damage Models, Monography N-79. Barcelona: CIMNE; 2003.

[34] Cervera M, Pelà L, Clemente R, Roca P. A crack-tracking technique for localized damage in quasi-brittle materials. Eng Fract Mech 2010;77:2431–50. doi:10.1016/j.engfracmech.2010.06.013.

[35] Saloustros S, Cervera M, Pelà L. Tracking multi-directional intersecting cracks in numerical modelling of masonry shear walls under cyclic loading. Meccanica 2018;53:1757–76. doi:10.1007/s11012-017-0712-3.

[36] Saloustros S, Pelà L, Cervera M, Roca P. An enhanced finite element macro-model for the realistic simulation of localized cracks in masonry structures: A large-scale application. Int J Archit Herit 2017;In press. doi:10.1080/15583058.2017.1323245.

[37] Domenge J. L'obra de la Seu. El procés de construcció de la catedral de Mallorca en el trescents. Palma de Mallorca. [In Catalan]: 1997.

[38] Domenge J. Análisis y estudio de los libros históricos de la Catedral. Documento No 3. Estudio, diagnóstico y peritación y en su caso planteamiento de actuaciones sobre el comportamiento constructivo- estructural de la catedral de Santa María, en la ciudad de Palma,. [In Spanish]: 2003.

[39] Foto Fitti. La Seu, 07001 Palma, Illes Balears, Spain. Wikimedia Commons 2012. https://commons.wikimedia.org/wiki/File:La_Seu,_07001_Palma,_Illes_Balears,_Spain_-_panoramio_(82).jpg.

[40] Roca P, González J. Estudio, diagóstico y peritación y en su caso planteamiento de actuaciones sobre el comportamiento constructivo-estructural de la catedral de Santa

Maria en la ciudad de Palma, isla de Mallorca (Baleares). Fase segunda (in Spanish). 2008.

[41] Pelà L, Bourgeois J, Roca P, Cervera M, Chiumenti M. Analysis of the Effect of Provisional Ties on the Construction and Current Deformation of Mallorca Cathedral. Int J Archit Herit 2016;10:418–37. doi:10.1080/15583058.2014.996920.

[42] Clemente R. Análysis estructural de edificios históricos mediante modelos localizados de fisuración. Universitat Politècnica de Catalunya (UPC-BarcelonaTech), 2006.

[43] Ruiz GM. Vulnerabilidad Sísmica para Edificios Históricos de Obra de Fábrica de Mediana y Gran Luz. Technical University of Catalonia (UPC-BarcelonaTech), 2007.

[44] Elyamani A, Mohamed A, Roca P. Integrated monitoring and structural analysis strategies for the study of large historical construction. Application to Mallorca cathedral. Universitat Politècnica de Catalunya, 2015.

[45] CEN. Eurocode 8 – Design of structures for earthquake resistance – Part 3: Assessment and retrofitting of buildings. EN 1998-3 2005.

[46] CNR-DT 212/2013. Guide for the Probabilistic Assessment of the Seismic Safety of Existing Buildings. Rome, Italy: 2014.

[47] Vendrell M, Giràldez P. Monestir de Poblet. Materials de les voltes de la nau de l'església. Barcelona, Spain: 2012.

[48] Roca P. Monasterio de Santa Maria de Poblet: Análisis de efectos estructurales causados por sobrecargas de uso de biblioteca en el edificio del antiguo dormitorio de los monjes en biblioteca. Barcelona, Spain: 2005.

[49] Instituto de la Construcción y del Cemento "Eduardo Torroja." P.I.E.T 70. Madrid, Spain: 1971.

[50] Italian Ministry of Infrastructure and Transport. LC-FC Norma Italiana (Circolare 2

Febbraio 2009 n.617). 2008.

[51] Saloustros S. Structural Analysis of the Church of the Poblet Monastery. Universitat Politècnica de Catalunya, 2013.

[52] Saloustros S, Pelà L, Cervera M, Roca P. An Enhanced Finite Element Macro-Model for the Realistic Simulation of Localized Cracks in Masonry Structures: A Large-Scale Application. Int J Archit Herit 2018;12:432–47. doi:10.1080/15583058.2017.1323245.

[53] Lourenço PB. Computational strategies for masonry structures. Delft University of Technology, 1996. doi:ISBN 90-407-1221-2.

[54] Roca P, Cervera M, Pelà L, Clemente R, Chiumenti M. Continuum FE models for the analysis of Mallorca Cathedral. Eng Struct 2013;46:653–70. doi:10.1016/j.engstruct.2012.08.005.

[55] Milani G, Valente M, Alessandri C. The narthex of the Church of the Nativity in Bethlehem: A non-linear finite element approach to predict the structural damage. Comput Struct 2018;207:3–18. doi:10.1016/j.compstruc.2017.03.010.

[56] Saloustros S, Pelà L, Roca P, Portal J. Numerical analysis of structural damage in the church of the Poblet monastery. Eng Fail Anal 2015;48:41–61. doi:10.1016/j.engfailanal.2014.10.015.

[57] Saloustros S, Pelà L, Contrafatto FR, Roca P, Petromichelakis I. Analytical Derivation of Seismic Fragility Curves for Historical Masonry Structures Based on Stochastic Analysis of Uncertain Material Parameters. Int J Archit Herit 2019;13:1142–64. doi:10.1080/15583058.2019.1638992.

[58] Fajfar P. Capacity spectrum method based on inelastic demand spectra. Earthq Eng Struct Dyn 1999;993:979–93.

[59] MIT 2019. Circolare del ministero delle infrastructure e dei trasporti, n.7 del 21 Gennaio

2019: "Istruzioni per l’applicazione dell’aggiornamento delle Norme tecniche per le costruzioni di cui al D.M. 17 gennaio 2018. Cons Super Dei Lav Pubblici GU n35 Del 11022019 2019.

[60] Federal Emergency Management Agency. HAZUS-MH MR4: Technical Manual, Vol. Earthquake Model. Washington DC: 2010.